

STATE FEEDBACK CONTROL OF A CAR AND BEAM PROTOTYPE

L.C. Camargo, V.H.S. Bispo, U.N.L.T. Alves, F.S.F. Ribeiro and R. Breganon*

Controle e Processos Industriais, Instituto Federal do Paraná - IFPR, BRAZIL
E-mail: ricardo.breganon@ifpr.edu.br

The Car and Beam prototype is a teaching piece of equipment, inspired by Ball and Beam systems. It consists of a beam supported in its center by means of a rotating axis installed in two rolling bearings, allowing the beam to rotate through the actuation of a servo motor. A car is coupled to this beam, and its displacement is measured using a linear encoder. This paper focuses on two key aspects: firstly, it offers a mathematical model of the Car and Beam system, and secondly, it outlines the development of a state-feedback tracking controller through pole placement to this system. To validate the modeling and control approach, we present simulation and experimental results using three different reference profiles: step, square wave, and sine wave. Our findings demonstrate the effectiveness of the control strategy in tracking predefined trajectories, both in simulation and with the physical prototype. In conclusion, this study highlights the efficacy of the methodology employed for mathematical modeling and the controller's design in the context of this specific application. The results indicate promising potential for further exploration in this domain.

Keywords: Car and Beam prototype, Ball and Beam, tracking controller, system model.

1. Introduction

The Car and Beam prototype is a teaching piece of equipment inspired by Ball and Beam systems. The primary objective of the Ball and Beam system is to maintain the ball's position on a beam by controlling the beam's angle (Garai and Balasubramanyam, [1]). Various control techniques have been introduced to manage this system.

In related literature, Ali *et al.* [2] and Csuresia *et al.* [3] utilized ARDUINO to implement a PID controller for Ball and Beam systems. Meanwhile, Garai and Balasubramanyam [1] employed a cascade PID controller to regulate the ball position. Aviles *et al.* [4] investigated a PD and a PID controller using an ESP32 as a data acquisition board.

Other controllers were also used to stabilize the ball in the desired position. Howimanporn *et al.* [5] introduced real-time monitoring and control a Ball and Beam system using a Fuzzy Predictive approach based on Programmable Logic Controller Network and Information Technologies. In the work by Zhang *et al.* [6], a Nonlinear Takagi-Sugeno Fuzzy Observer Design was presented. Zaare and Soltanpour [7] developed a position control strategy for a Ball and Beam system, incorporating a State-Disturbance Observer-Based Adaptive Fuzzy Sliding Mode Control to handle matched and mismatched uncertainties. Furthermore, Rosa *et al.* [8] implemented a Cascaded LQR-FLC (Linear Quadratic Regulator – Feedback Linearization Controller).

Throughout our research, it became evident that numerous studies explored the application of control techniques using Ball and Beam prototypes. However, there is a limited body of work that focuses on similar Car and Beam prototypes like the one under investigation in this study. For instance, Yeom [9] utilized a U-profile beam to regulate the wheel's position. The author achieved this by implementing a PID controller, with controller gains determined through the particle swarm optimization algorithm. Additionally, Niro *et al.* [10] introduced a real-time tracking system for a modified Ball and Beam system, employing a DC motor as the

* To whom correspondence should be addressed

actuator. Considering this, the Car and Beam prototype emerges as a promising subject with significant potential for further exploration.

The state-feedback control using the pole placement technique employed in this study enables the positioning of a dynamic system's poles at specific locations to achieve the desired performance of the closed-loop system (Yoneyama, [11]). A range of prior studies has used the pole placement technique in combination with other control methods, conducting extensive simulations to explore the behavior of the different dynamic systems. For instance, Breganon *et al.* [12] designed a pole placement controller for both linear and nonlinear models of a rotational inverted pendulum, commonly referred to as Furuta pendulum. Aguiar and Lordelo [13] applied this technique to control the position of a direct current electric motor connected to an uncertain load. Guo *et al.* [14] proposed a robust finite-time trajectory tracking control strategy for wheeled mobile robots dealing with parametric uncertainties and disturbances. In this study, to mitigate the impact of lumped uncertainties, a nonlinear extended state observer was employed to estimate unknown states and uncertainties, with the associated coefficients tuned using the pole placement technique. Abdulwahhab [15] utilized pole placement control in simulating a magnetic levitation system. Additionally, in the works of Kim *et al.* [16], Souza and Souza [17], and Silva and Prado [18], the pole placement technique was applied to dynamic models of an autonomous underwater vehicle, a satellite attitude control system, and an active suspension system manufactured by Quanser, respectively.

The state feedback-based pole placement technique also produced significant implementation outcomes. For instance, Bispo *et al.* [19] employed this approach to regulate the angular position of a Propeller and Beam system. Shang *et al.* [20] utilized a method that combines a neural network RBF (Radial Basis Function) and pole placement to control a flexible servo manipulator system and reduce rotation angle fluctuations. Additionally, Zhu and Li [21] introduced a robust fault estimation design for an experimental 3 DOF helicopter system, taking into account actuator saturation and utilizing the pole placement technique to fine-tune the transient response of estimation errors.

This paper focuses on two primary aspects: developing the mathematical model of a Car and Beam prototype and designing a state-feedback tracking controller through pole placement to manage the car's position along the beam's length. Note that this approach differs this paper from Yamanaka *et al.* [22], which control this prototype using a PID controller without obtaining a system model. Subsequently, we analyzed simulation and experimental results to assess the effectiveness of the proposed methodology in this context.

The structure of the paper is as follows. Section 2 covers of the Car and Beam prototype design. Section 3 covers the modeling of the prototype. Section 4 presents the state-feedback tracking control for the prototype. In Section 5, we explore pole placement concepts. Section 6 is dedicated to discussing the results obtained. Finally, Section 7 presents the study's conclusions.

2. Car and Beam prototype

The Car and Beam prototype considered in this paper consists of a horizontal structural beam of aluminum that measures $20 \times 20 \text{ mm}$, with a V-slot design and a length of 500 mm . This beam is securely affixed at its center through a stainless-steel shaft, which has an 8 mm diameter. Two rolling bearings support this central shaft, enabling the beam's rotation. Attached to the beam is a car equipped with four ball-bearing pulleys responsible for facilitating its movement, as detailed by Yamanaka *et al.* [22]. The prototype, as shown in Fig.1. Important components of the setup are indicated in Fig.1 by corresponding numbers.

To operate the prototype, we use an Intel Core 2 Duo E8400 computer ① running at 3 GHz , equipped with 3 GB of RAM. This computer has Matlab/Simulink software installed along with the Simulink Real-Time toolbox. Additionally, we utilize a National Instruments PCI-6221 hardware component for receiving and transmitting data through a block of connectors ②. For the angular movement of the system, we employ a TowerPro MG995 servo motor ③, which offers a variable torque range between 9.4 kg cm and 11 kg cm for voltages ranging from 4.8 V to 6 V , respectively. This servo motor is connected to the beam via an aluminum rod, and its angular variation is controlled through a Pulse Width Modulation (PWM) signal.

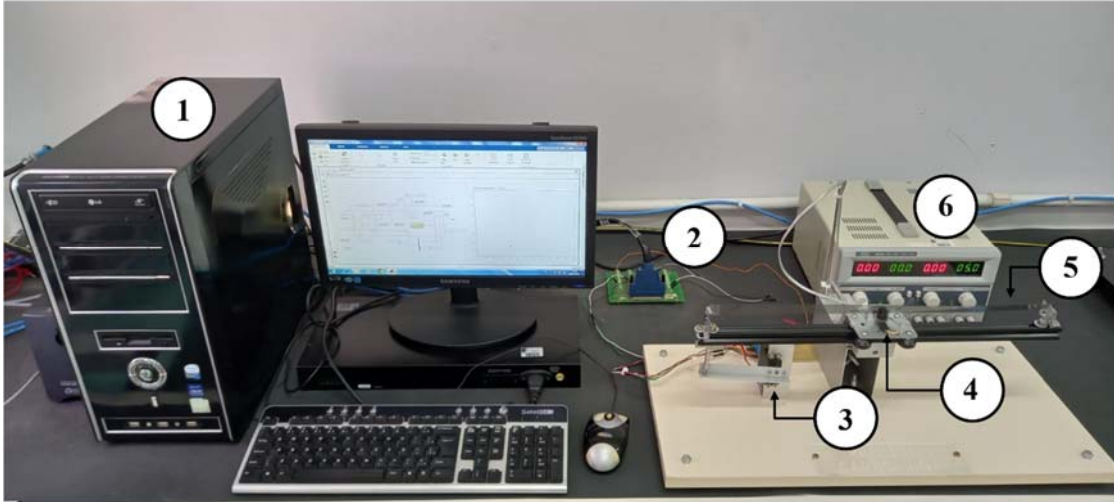


Fig.1. Car and Beam prototype setup.

The prototype includes a linear encoder, a H9720 model from AVAGO, installed on the car to provide position feedback along the length of the beam (4). This linear encoder is connected to a linear strip (5) with a resolution of 150 Lpi (Lines per inch). The servo motor and linear encoder are powered by a DC power supply (6).

3. Car and Beam modeling

We derive the differential equations describing the dynamics of a system by applying the relevant physical laws that govern the process, as outlined by Dorf and Bishop [23]. Figure 2 shows a diagram of the Car and Beam system and the forces influencing the car's motion, where the moment of inertia of the wheels was neglected because it has small values. Applying Newton's second law, we obtain the following differential equation:

$$m\ddot{x}(t) - mg\sin(\theta(t)) - F_t(t) = 0, \quad (3.1)$$

where m is the mass of the car, $g = 9810\text{ mm/s}^2$ is the acceleration of gravity, F_t is the frictional force of the car.

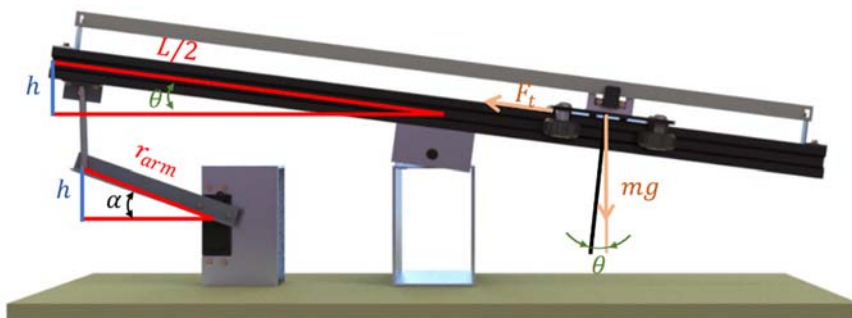


Fig.2. Car and Beam prototype and its acting forces.

Disregarding the frictional force on the wheels of the car $F_t(t)$, to simplify the model, it follows that

$$\begin{aligned}
m\ddot{x}(t) - mg\sin(\theta(t)) &= 0, \\
m\ddot{x}(t) &= mg\sin(\theta(t)), \\
\ddot{x}(t) &= g\sin(\theta(t)).
\end{aligned} \tag{3.2}$$

Note that the angle θ differs from the servo motor axis angle α . To convert the beam angle into the servo motor angle, we utilize the relationships illustrated in Fig.2, which leads to the following equations:

$$\sin(\alpha) = \frac{h}{r_{arm}}, \tag{3.3}$$

$$\sin(\theta) = \frac{h}{L/2}, \tag{3.4}$$

where $r_{arm} = 105 \text{ mm}$ is the length of the arm attached to the servo motor, and $L = 500 \text{ mm}$ is the total length of the beam. Thus, from Eqs (3.3)-(3.4), we have

$$\sin(\alpha)r_{arm} = \sin(\theta)\frac{L}{2} = h, \tag{3.5}$$

$$\sin(\theta) = \frac{2\sin(\alpha)r_{arm}}{L}.$$

Substituting Eq.(3.5) into Eq.(3.2), it yields

$$\ddot{x}(t) = g \frac{2\sin(\alpha)r_{arm}}{L}. \tag{3.6}$$

By introducing the new variable $\alpha = \sin^{-1}u$, where u is the system's input, from Eq.(3.6), we obtain

$$\ddot{x}(t) = \frac{2gr_{arm}}{L}u(t). \tag{3.7}$$

Choosing the state variables as the position $x = x_1$ and the velocity $\dot{x} = x_2$ of the car, from Eq.(3.7) and the parameters described below Eqs (3.1) and (3.4), we represent the dynamics of the Car and Beam system by

$$\dot{x}(t) = Ax(t) + Bu(t), \quad y(t) = Cx(t), \tag{3.8}$$

$$x(t) = \begin{bmatrix} x_1(t) \\ x_2(t) \end{bmatrix}, \quad A = \begin{bmatrix} 0 & I \\ 0 & 0 \end{bmatrix}, \quad B = \begin{bmatrix} 0 \\ 4120.2 \end{bmatrix} \quad \text{and} \quad C = [I \quad 0].$$

From the state space representation in Eq.(3.8), it is possible to verify the controllability of the system and design a tracking controller for it, as described in Sections 4 and 5.

4. Tracking control

The tracking control block diagram is shown in Fig.3 (Ogata, [24]; D'Azzo and Houpis [25]).

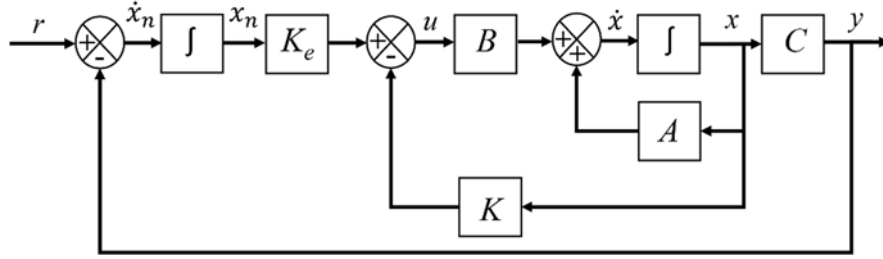


Fig.3. Tracking control diagram (adapted from D'Azzo and Houpis [25]).

From the block diagram in Fig.3, we obtain

$$\dot{x}_n(t) = r(t) - Cx(t), \quad (4.1)$$

$$u(t) = -Kx(t) + K_e x_n(t) = -[K \quad -K_e] \begin{bmatrix} x(t) \\ x_n(t) \end{bmatrix} = -\hat{K} \begin{bmatrix} x(t) \\ x_n(t) \end{bmatrix}. \quad (4.2)$$

By representing the dynamics in Eq.(3.8) together with the dynamics in Eq.(4.1), we have

$$\begin{bmatrix} \dot{x}(t) \\ \dot{x}_n(t) \end{bmatrix} = \begin{bmatrix} A & 0 \\ -C & 0 \end{bmatrix} \begin{bmatrix} x(t) \\ x_n(t) \end{bmatrix} + \begin{bmatrix} B \\ 0 \end{bmatrix} u(t) + \begin{bmatrix} 0 \\ I \end{bmatrix} r(t). \quad (4.3)$$

Assuming that the system is stable and that $x(\infty)$, $x_n(\infty)$ and $u(\infty)$ tend to constant values, in steady state, from Eq.(4.3), we obtain (Ogata, [24])

$$\begin{bmatrix} \dot{x}(\infty) \\ \dot{x}_n(\infty) \end{bmatrix} = \begin{bmatrix} A & 0 \\ -C & 0 \end{bmatrix} \begin{bmatrix} x(\infty) \\ x_n(\infty) \end{bmatrix} + \begin{bmatrix} B \\ 0 \end{bmatrix} u(\infty) + \begin{bmatrix} 0 \\ I \end{bmatrix} r(\infty). \quad (4.4)$$

Considering $r(t)$ a step input, one has $r(\infty) = r(t) = r$ for all $t > 0$. Thus, subtracting Eq.(4.3) from Eq.(4.4) results in

$$\begin{bmatrix} \dot{x}(t) - \dot{x}(\infty) \\ \dot{x}_n(t) - \dot{x}_n(\infty) \end{bmatrix} = \begin{bmatrix} A & 0 \\ -C & 0 \end{bmatrix} \begin{bmatrix} x(t) - x(\infty) \\ x_n(t) - x_n(\infty) \end{bmatrix} + \begin{bmatrix} B \\ 0 \end{bmatrix} [u(t) - u(\infty)]. \quad (4.5)$$

Let

$$\hat{x}(t) = \begin{bmatrix} x_e(t) \\ x_{ne}(t) \end{bmatrix}, \quad x_e(t) = x(t) - x(\infty), \quad x_{ne}(t) = x_n(t) - x_n(\infty), \quad \hat{u}(t) = u(t) - u(\infty),$$

$$\hat{A} = \begin{bmatrix} A & 0 \\ -C & 0 \end{bmatrix}, \quad \hat{B} = \begin{bmatrix} B \\ 0 \end{bmatrix} \quad \text{and} \quad \hat{C} = [C \quad 0]$$

from Eq.(3.8) and Eq.(4.5), it follows that

$$\dot{\hat{x}}(t) = \hat{A}\hat{x}(t) + \hat{B}\hat{u}(t), \quad y(t) = \hat{C}\hat{x}(t), \quad (4.6)$$

$$\hat{A} = \begin{bmatrix} 0 & 1 & 0 \\ 0 & 0 & 0 \\ -1 & 0 & 0 \end{bmatrix}, \quad \hat{B} = \begin{bmatrix} 0 \\ 4120.2 \\ 0 \end{bmatrix}, \quad \hat{C} = [1 \ 0 \ 0]. \quad (4.7)$$

5. Pole placement

State feedback involves utilizing information about all state variables of the system model, enabling the placement of closed-loop system poles as desired. For this placement to be carried out in an arbitrary manner, it is necessary and sufficient that the controllability matrix $C_o = [B \ AB \ A^2B \ \dots \ A^{(n-1)}B]$ has a rank equal to n , where n is the order of the mathematical model. In this case, we say that the system is controllable (Nise, [26]).

Calculating the controllability matrix for the system in Eqs (4.6)-(4.7), we have

$$C_o = [\hat{B} : \hat{A}\hat{B} : \hat{A}^2\hat{B}], \quad (5.1)$$

$$C_o = \begin{bmatrix} 0 & 4120.2 & 0 \\ 4120.2 & 0 & 0 \\ 0 & 0 & -4120.2 \end{bmatrix}, \quad (5.2)$$

$$\det(C_o) = 6.9945 \times 10^{10} \neq 0. \quad (5.3)$$

In Eq.(5.3), the controllability matrix of the system in Eqs (4.6)-(4.7) has a non-zero determinant. Then, this system is controllable, which, according to Nise [26], enables designing a state-feedback controller in state space with pole placement.

By substituting the control law from Eq.(4.2) into the state space model presented in Eq.(4.3), the dynamics become:

$$\dot{\hat{x}}(t) = (\hat{A} - \hat{B}\hat{K})\hat{x}(t) + \hat{B}r, \quad (5.4)$$

$$y = \hat{C}\hat{x}(t).$$

We can see that the matrix $(\hat{A} - \hat{B}\hat{K})$ serves as the state matrix for the closed-loop system. Consequently, modifying the values of the gain \hat{K} leads to changes in the eigenvalues of this matrix, thereby influencing the system's dynamics.

The characteristic equation of the closed-loop system is computed as follows:

$$\det(sI - \hat{A} + \hat{B}\hat{K}) = 0. \quad (5.5)$$

Suppose we have a set of desired poles denoted as $P=[\gamma_1 \gamma_2 \dots \gamma_n]$. In that case, the desired characteristic equation for the system can be represented as $\alpha_c=(s-\gamma_1)(s-\gamma_2)\dots(s-\gamma_n)=0$. Consequently, it is feasible to determine the values of $K=[K_1 \ K_2 \ \dots \ K_n]$ that make the closed-loop characteristic equation equal to the desired characteristic equation, resulting in:

$$\det(sI-\hat{A}+\hat{B}\hat{K})=(s-\gamma_1)(s-\gamma_2)\dots(s-\gamma_n). \quad (5.6)$$

Alternative methods for determining the gain \hat{K} for implementing pole placement can be found in Ogata [24] and Nise [26].

6. Results and discussions

The control scheme of the Car and Beam system is shown in Fig.4. A linear encoder measures the car's position. This variable is derived with the help of a derivative filter described by $F(s)=\frac{10s}{s+10}$, in order to mitigate noise and obtain the car's velocity. The position of the car is also compared with the reference r , generating the error signal, which is integrated to create the variable x_n , as explained in the diagram in Fig.3. The values of these three variables are used to produce the control signal u . After that, the value of the control signal u is converted to the servo motor axis angle, α , and from this angle to the corresponding PWM value. The PWM signal is used to drive the servo motor. The servo motor acts on the system, changing the angle of the beam and, consequently, moving the car.

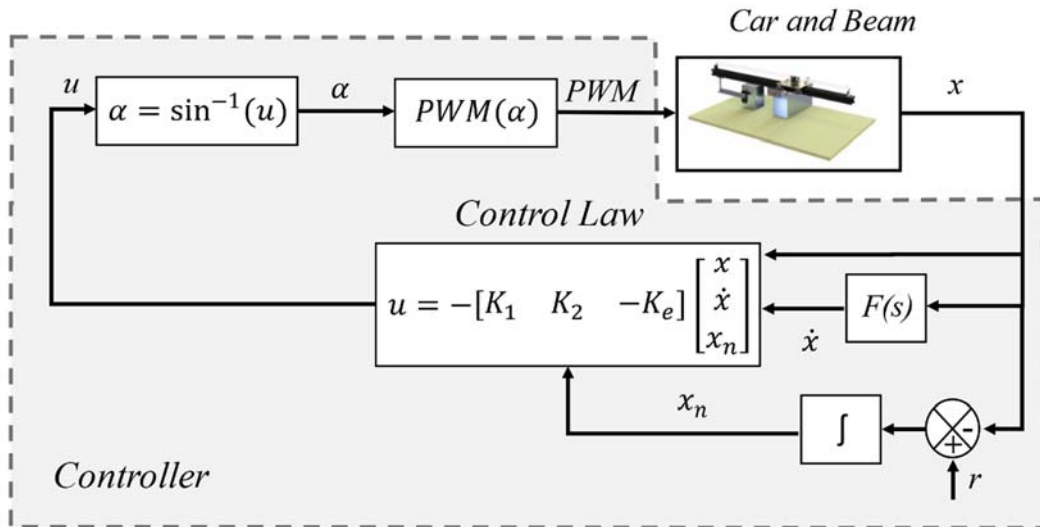


Fig.4. Car and Beam control system diagram.

The mathematical model, given in Eq.(3.7), utilizes $u = \sin(\alpha)$ as the control input, where α represents the angle in the servo motor axis. As shown in Fig.4, a PWM signal is used to control the Car and Beam prototype through servo motor activation. We assume a linear relationship between the axis angle and the PWM signal for the angle-to-PWM conversion. Therefore, we conducted tests on the prototype to establish the relationship between the PWM signal and the angle in the servo motor. The resulting data is illustrated in Fig.5.

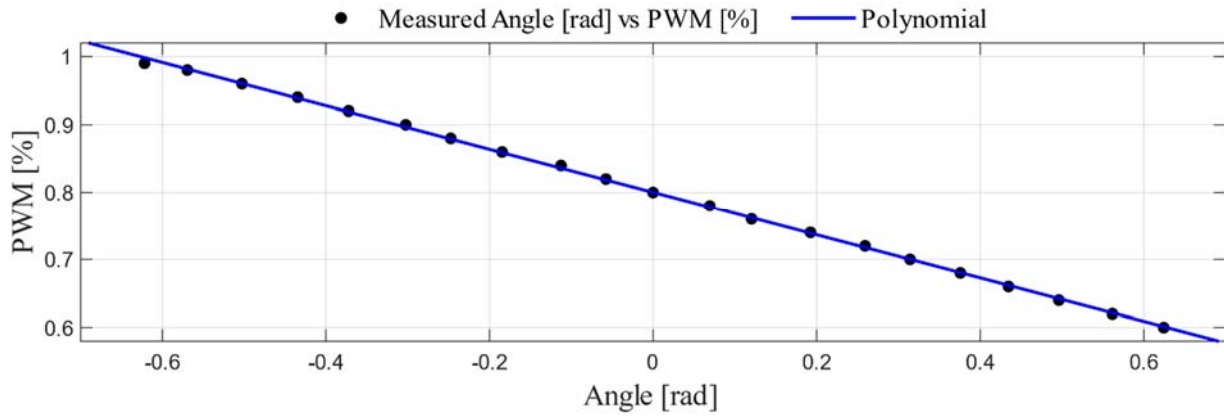


Fig.5. Relationship between measured angle in the servo motor axis and the PWM signal.

The polynomial that describes the relationship between the measured angle and the PWM signal is presented in Eq.(6.1)

$$PWM = -0.3185\alpha + 0.8002. \quad (6.1)$$

As described in Sec.5, it is necessary to choose the desired polos to design the feedback gain \hat{K} . In this paper, the poles were chosen based on simulations and experimental tests with the prototype. It is important to note that the poles must be on the left side of the complex plane (real part less than zero). We choose the following poles

$$P = [-4 \quad -2.5 \quad -0.5]. \quad (6.2)$$

With the poles from Eq.(6.2) and the matrices from Eq.(4.7), the Matlab 'place' command was used to calculate the tracking control gains. The values found were: $K = [K_1 \quad K_2] = [0.0032 \quad 0.0017]$ and $K_e = [-0.0012]$.

We conducted three simulations and tests using the prototype to validate whether the mathematical model accurately reflects the system's dynamics. Additionally, we assessed whether the tracking control via pole placement can effectively move the car to the desired position and stabilize the system.

The first condition tested in this work was a step-like reference described by Eq.(6.3)

$$r_{step}(t) = \begin{cases} 0 \text{ mm}, & 0 \text{ s} \leq t < 5 \text{ s}, \\ 90 \text{ mm}, & 5 \text{ s} \leq t < 30 \text{ s}, \\ 180 \text{ mm}, & 30 \text{ s} \leq t < 60 \text{ s}. \end{cases} \quad (6.3)$$

Figure 6 shows that the controller exhibited a similar response in simulation and in experimentation. This figure also displays the control action guiding the system to follow the specified step-like reference. Notably, during the time intervals between 12 s to 30 s and 38 s to 60 s, changes in the control signal are evident during the experiment, even when the car is stabilized in the desired position. This phenomenon can

be attributed to the dead zone of the servo motor, preventing its angular variation within the system. Further investigation of this phenomenon is left for future work.

The second test considered a square wave reference given by Eq.(6.4)

$$r_{sw}(t) = \begin{cases} 180 \text{ mm}, & 5 \text{ s} \leq t < 30 \text{ s}, \\ 0 \text{ mm}, & 30 \text{ s} < t < 45 \text{ s}, \\ 180 \text{ mm}, & 45 \text{ s} \leq t < 70 \text{ s}, \\ 0 \text{ mm}, & 70 \text{ s} < t < 85 \text{ s}, \\ 180 \text{ mm}, & 85 \text{ s} \leq t < 110 \text{ s}, \\ 0, & \text{otherwise.} \end{cases} \quad (6.4)$$

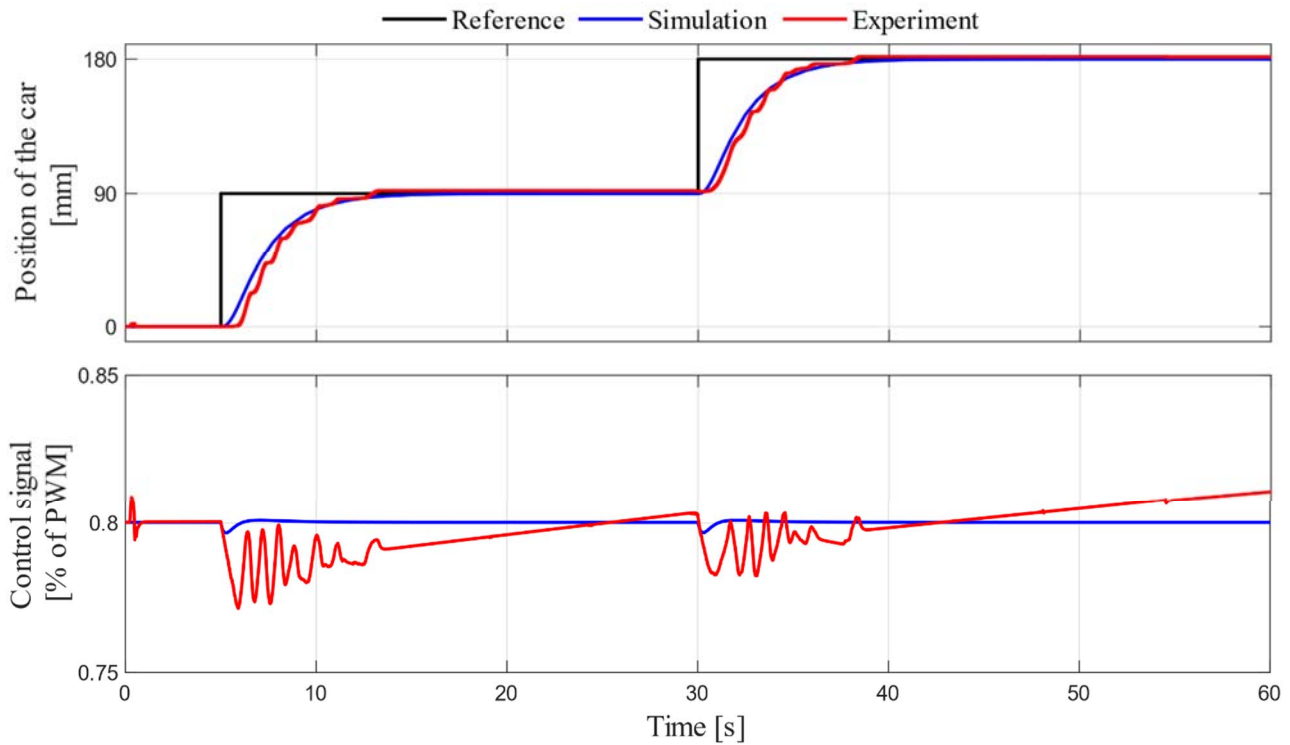


Fig.6. System response and control action used to track the reference Eq.(6.3).

The response for this second reference can be seen in Fig.7, where it is possible to observe that the closed-loop system demonstrated a similar response in both the simulation and the experiment. The controller generated an effective control action to ensure the car tracks the desired square wave reference. In the control action, at moments 15 s to 29 s and 52 s to 69 s, there was also a change in the signal due to the same circumstances of the servo motor dead zone.

The third and final test was performed applying a sine wave reference described by Eq.(6.5).

$$r_{sin}(t) = [90 \sin(0.2\pi t) + 90] \text{mm}. \tag{6.5}$$

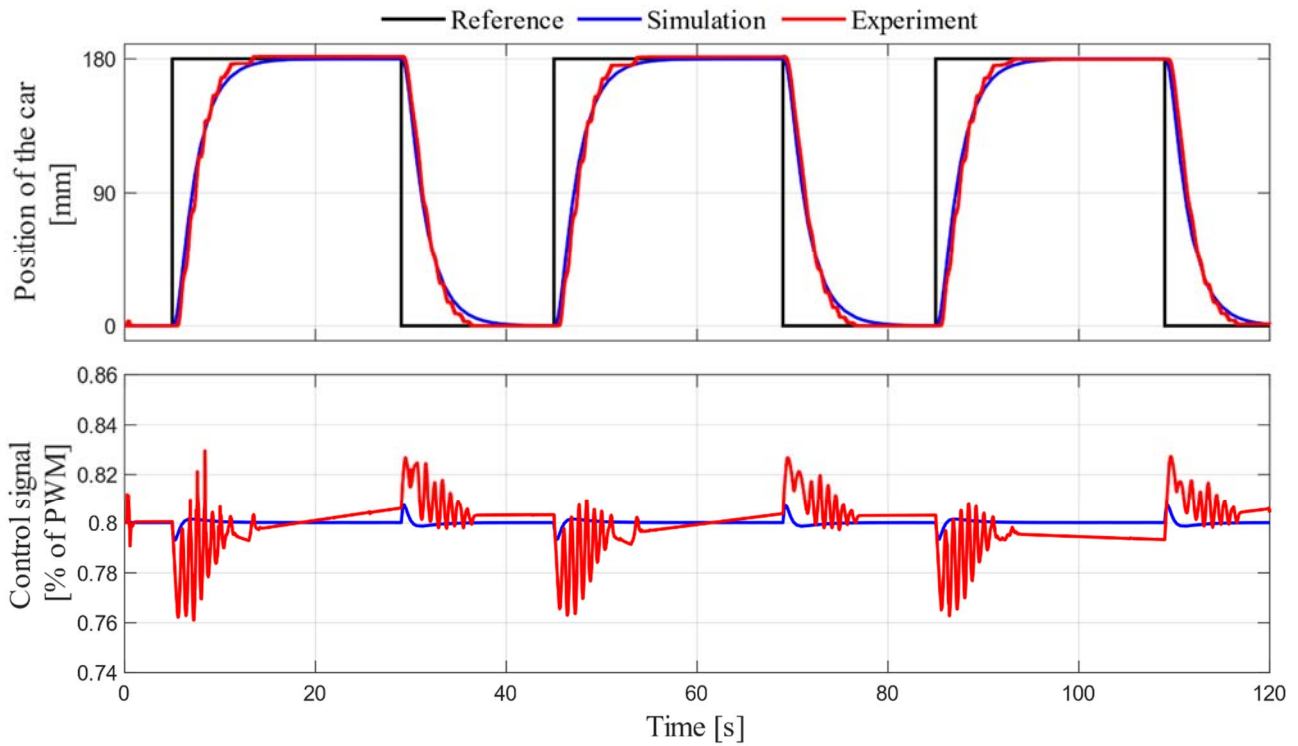


Fig.7. System response and control action used to track the reference Eq.(6.4).

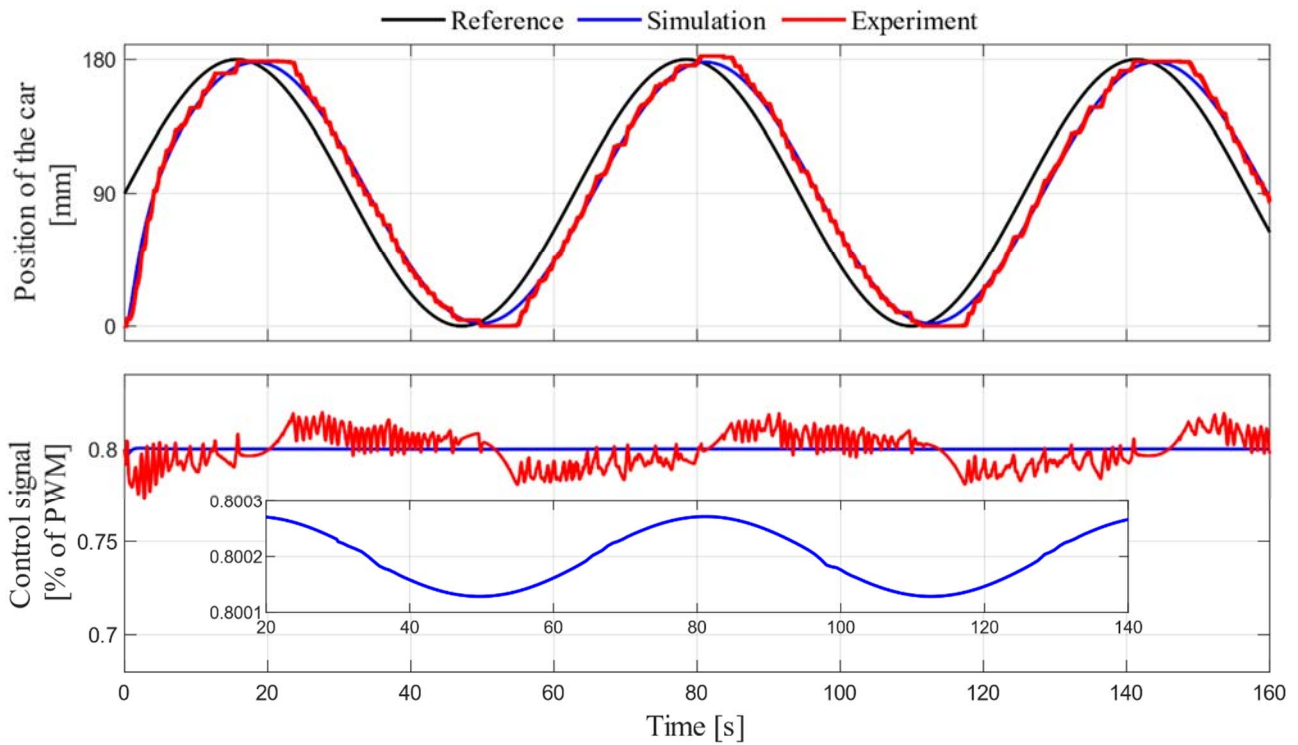


Fig.8. System response and control action used to track the reference Eq.(6.5).

In Figure 8, it is noticeable that there was an error in the system's response both in the simulation and the experiment. This error is due to the reference being a sine wave with a non-zero derivative, which differs from the reference used in developing the controller described in Sec. 4. This error can be made smaller by choosing the eigenvalues of the closed-loop system with more negative real parts (Dorf, [23]; Ogata, [24]). Another important detail is that the reference starts at 90 mm , while the car begins at 0 mm , as indicated in the response. A notable difference is observed in the control signal, which appears much smaller in the simulation compared to the experiment. To highlight the variation of the control signal in the simulation, an enlargement was carried out from the moment 20 s to 140 s , also shown in Fig.8.

7. Conclusions

This paper presented a methodology for modeling and controlling a Car and Beam prototype. The obtained model is nonlinear, and we introduced a change of variable to linearize the system dynamics. The experimental prototype allows for measuring the car's position, which is processed to control the car's movement. The position is acquired through a linear encoder and undergoes a derivative filter to obtain the car's velocity while reducing noise. The error signal is generated by comparing the car's position with a reference, and this error is integrated to create a new control variable, x_n . These three variables are utilized to generate a control signal, subsequently converted to a PWM signal to control the axis angle of the servo motor, moving the beam and, consequently, the car to the desired position. The conversion from the servo motor angle to the PWM signal was determined by a linear function derived through tests with the prototype. By examining the response characteristics presented in Figs 6-8, it is possible to verify that the mathematical model aligns with the dynamics of the real prototype, as the rise and accommodation times were similar.

From the obtained simulation and experimental results, it is concluded that the methodology used to design the tracking control via pole placement was satisfactory for this application. The controller effectively tracked the desired reference in all three conducted tests. For future work, we plan to explore other control techniques and compare their performance with the results presented in this paper.

Acknowledgements

The authors would like to thank the IFPR, Jacarezinho, Paraná, Brazil, for their financial support in the development of this work.

Nomenclature

- A – state matrix
- B – input matrix
- \hat{A} – state matrix for the augmented dynamics
- \hat{B} – input matrix for the augmented dynamics
- C – output matrix
- \hat{C} – output matrix for the augmented dynamics
- C_o – controllability matrix
- $F(s)$ – derivative filter
- F_t – friction force acting on the movement of the car
- g – acceleration of gravity
- h – height in relation to angle
- K – state gain
- K_e – integrator gain

- \hat{K} – controller gain
 K_1 – position gain
 K_2 – velocity gain
 L – total beam length
 m – car mass
 P – system poles
 r – system reference
 r_{arm} – length of arm attached to the motor
 r_{sin} – sine wave reference
 r_{step} – step-like reference
 r_{sw} – square wave reference
 $\dot{\hat{x}}$ – augmented state vector derivative
 u – system control signal
 \hat{u} – difference between the actual control signal and its steady state value
 x – car position
 \hat{x} – augmented state vector
 \dot{x} – car velocity
 \ddot{x} – car acceleration
 x_1, x_2 – state variables
 x_e – difference between the actual state of the system and its steady state value
 x_n – new state variable consisting of the difference between the reference and the output of the system
 x_{ne} – difference between the new state variable and its steady state value
 y – system output
 α – servo motor axis angle
 θ – beam angle

References

- [1] Garai S. and Balasubramanyam N.H. (2020): *Tuning of Ball and Beam system using cascade control.*–International Journal of Engineering and Management Research, vol.10, No.4, pp.56-59. Doi: <https://doi.org/10.31033/ijemr.10.4.9>
- [2] Ali A.T., Ahmed A.M., Almahdi H.A., Osama A.T. and Naseraldeem A. (2017): *Design and implementation of Ball and Beam System using PID controller.*– Journal of Electrical and Computer Engineering, vol.1, pp.1-9.
- [3] Csurscia P.Z., Bhandari P. and Troyer T.D. (2022): *Development of a low-cost PID setup for engineering technology students.*– IFAC Paper Online, Science Direct, vol.55-54, pp.213-218.
- [4] Aviles M., Rodríguez-Reséndiz J., Pérez-Ospina J. and Lara-Mendoza O. (2023): *A comprehensive methodology for the development of an open-source experimental platform for control courses.*– Technologies, MDPI, vol.11, p.25. Doi: <https://doi.org/10.3390/technologies11010025>.
- [5] Howimanporn S., Chookaew S. and Silawatchananai C. (2022): *Monitoring and controlling of a real-time ball beam fuzzy predicting based on PLC network and information technologies.*– Journal of Advances in Information Technology, vol.13, No.1, pp.1-8. Doi: 10.12720/jait.13.1.1-8.
- [6] Zhang W., Bai L., Zhang S. and Pan J. (2021): *Nonlinear Takagi-Sugeno fuzzy observer design for a Ball and Beam system.*– IFAC Paper Online, Science Direct, vol.54, No.54, pp.201-205. Doi: 10.1016/j.ifacol.2021.10.034.

- [7] Zaare S. and Soltanpour M.R. (2020): *The position control of the Ball and Beam system using state-disturbance observer-based adaptive fuzzy sliding mode control in presence of matched and mismatched uncertainties.*– Mechanical System and Signal Processing, pp.1-23. Doi: <https://doi.org/10.1016/j.ymssp.2020.107243>.
- [8] Rosa M.R., Romdloy M.Z. and Trilaksono B.R. (2023): *The Ball and Beam System: cascaded LQR-FLC design and implementation.*– International Journal of Control, Automation, and Systems, vol.21, No.1, pp.201-207, Doi: <http://dx.doi.org/10.1007/s12555-021-0542-x>.
- [9] Yeom K. (2018): *Intelligent controller modelling for steerable robotic bar using bio-inspired control synthesis.*– Microsystem Technologies, pp.1493-1504, Doi: <doi.org/10.1007/s00542-018-4033-9>.
- [10] Niro L., Kaneko E.H., Mollon M.F., Chaves W.S. and Montezuma M.A.F. (2017): *Control of a modified Ball and Beam system using tracking system in real time with a DC motor as an actuator.*– International Journal of Advanced Engineering Research and Science (IJAERS), vol.4, No.12, pp.99-107, Doi: <https://dx.doi.org/10.22161/ijaers.4.12.17>.
- [11] Yoneyama T. (2022): *Engenharia de Controle: Teoria e Prática*. 1 ed. São Paulo: Blucher.
- [12] Breganon R., Alves U.N.L.T., Pivovar L.E., de Almeida J.P.L.S., Ribeiro F.S.F., Barbara G.V. and Mendonça M. (2020): *A study on control using state feedback with pole placement in a Furuta pendulum.*– Brazilian Journal of Development, vol.6, No.6, pp.36373-36390, doi:10.34117/bjdv6n6-253.
- [13] Aguiar A. R. and Lordelo A.D.S. (2021): *Interval analysis-based design of a robust DC electric motor position controller coupled to an uncertain load (in Portuguese).*– Journal of Production and Automation (JPAUT) ISSN 2595-9573, vol.4, No.1, pp.23-37, Retrieved from <https://jpaut.com.br/index.php/jpaut/article/view/45>
- [14] Guo Y., Yu L. and Xu J. (2019): *Robust finite-time trajectory tracking control of wheeled mobile robots with parametric uncertainties and disturbances.*– Journal of Systems Science and Complexity, vol.32, pp.1358-1374.
- [15] Abdulwahhab O.W. (2020): *Design of an adaptive state feedback controller for a magnetic levitation systems.*– International Journal of Electrical and Computer Engineering, vol.10, pp.4782-4788.
- [16] Kim E., Fan S., Bose N. and Nguyen H. (2021): *Current estimation and path following for an autonomous underwater vehicle (AUV) by using a high-gain observer based on an AUV dynamic model.*– International Journal of Control, Automation and Systems, vol.19, pp.478-490.
- [17] Souza A. and Souza L. (2021): *Comparison of the satellite attitude control system design using the H_∞ method and H_∞/MLI with pole allocation considering the parametric uncertainty.*– WSEAS Transactions on Circuits and Systems, vol.20, pp.88-95, Doi:10.37394/23201.2021.20.12
- [18] Silva J.M. and Prado M.L.M. (2019): *Pole allocation controller applied to an active suspension system (in Portuguese).*– In Congresso Brasileiro de Automática-CBA, vol.1, No.1.
- [19] Bispo V.H.S., Camargo L.C., Yamanaka H.F., Bispo C.A.S., Breganon R. and Alves U.N.L.T. (2022): *Control of a propeller-beam system using servo system via pole placement.*– Revista Mundi Engenharia, Tecnologia e Gestão, Paranaguá, vol.7, No.7, pp.463-471, Doi: 10.21575/25254782rmetg2022vol7n72354.
- [20] Shang D., Li X., Yin M. and Li F. (2021): *Control method of flexible manipulator servo system based on a combination of RBF neural network and pole placement strategy.*– Mathematics, vol.9, No.8, p.896.
- [21] Zhu X. and Li D. (2021): *Robust fault estimation for a 3-DOF helicopter considering actuator saturation.*– Mechanical Systems and Signal Processing, vol.155, Article No.107624.
- [22] Yamanaka H.F., Bispo C.A.S., Camargo L.C., Bispo V.H.S., Alves U.N.L.T. and Breganon R. (2022): *Construction and PID control of an experimental Car-Beam platform.*– Revista Mundi Engenharia, Tecnologia e Gestão, vol.7, No.7, pp.460-471, dDoi: 10.21575/25254782rmetg2022vol7n72342.
- [23] Dorf R. C. and Bishop, R. H. (2022): *Modern Control Systems.*– 13 ed. New Jersey: Pearson.
- [24] Ogata K. (2010): *Modern Control Engineering.*– 5 ed. New Jersey: Pearson Hall.
- [25] D’Azzo J. J. and Houpis C. H. (1988): *Linear Control System Analysis and Design: Conventional and Modern.*– 3 ed. New York: McGraw-Hill Publishing Company.
- [26] Nise N. S. (2019): *Control Systems Engineering.*– 8 ed. California: John Wiley & Sons, Inc.

Received: February 12, 2024

Revised: April 18, 2024